Colors of Centaurs

Stephen C. Tegler
Northern Arizona University

James M. Bauer
Jet Propulsion Laboratory

William Romanishin
University of Oklahoma

Nuno Peixinho
Grupo de Astrofisica da Universidade de Coimbra

Minor planets on outer planet-crossing orbits, called Centaur objects, are important members of the solar system in that they dynamically link Kuiper belt objects to Jupiter-family comets. In addition, perhaps 6% of near-Earth objects have histories as Centaur objects. The total mass of Centaurs (10^{-4} $M_{\oplus}$) is significant, about one-tenth of the mass of the asteroid belt. Centaur objects exhibit a physical property not seen among any other objects in the solar system, their B–R colors divide into two distinct populations: a gray and a red population. Application of the dip test to B–R colors in the literature indicates there is a 99.5% probability that Centaurs exhibit a bimodal color distribution. Although there are hints that gray and red Centaurs exhibit different orbital elements, application of the Wilcoxon rank sum test finds no statistically significant difference between the orbital elements of the two color groups. On the other hand, gray and red Centaurs exhibit a statistically significant difference in albedo, with the gray Centaurs having a lower median albedo than the red Centaurs. Further observational and dynamical work is necessary to determine whether the two color populations are the result of (1) evolutionary processes such as radiation-reddening, collisions, and sublimation or (2) a primordial, temperature-induced, composition gradient.

1. INTRODUCTION

October 18, 1977, marks the discovery of the first minor planet with a perihelion distance far beyond the orbit of Jupiter (*Kowal,* 1979). Because the minor planet was on an orbit largely lying between Saturn and Uranus, Kowal named his discovery after the Centaur Chiron, son of Kronos (Saturn) and grandson of Uranus. Fifteen years would elapse before the discovery of the next Centaur (1992 AD; 5145 Pholus) by the Spacewatch asteroid search project (*Scotti,* 1992). There are now several dozen Centaurs known.

There is no generally agreed upon definition of the term Centaur in the literature. The term is frequently and loosely defined as a minor planet on an outer-planet-crossing orbit. Here, we use a precisely constrained definition for Centaur given by the Minor Planet Center, an object on an orbit with semimajor axis, a, less than Neptune's orbit at 30.1 AU and a perihelion distance, q, larger than Jupiter's orbit at 5.2 AU. As of September 30, 2006, there are 39 objects in the Lowell Observatory Deep Ecliptic Survey database and 62 objects in the Minor Planet Center database with $q > 5.2$ AU and $a < 30.1$ AU.

Planetary perturbations and mutual collisions in the Kuiper belt are probably responsible for the ejection of objects from the Kuiper belt onto Centaur orbits. The Kuiper belt dynamical classes (e.g., Plutinos, classical objects, scattered disk objects) that are the sources of Centaurs are unknown. Numerical simulations of Neptune's gravitational influence on Kuiper belt objects (KBOs) indicate that more objects are perturbed onto orbits with larger semimajor axes, while fewer objects are perturbed onto orbits with smaller semimajor axes, i.e., Centaur orbits (*Levison and Duncan,* 1997). Because Centaurs cross the orbits of the outer planets, they are dynamically unstable, with lifetimes ~10^6 yr (*Tiscareno and Malhotra,* 2003; *Horner et al.,* 2004). Some Centaurs evolve into Jupiter-family comets, others are ejected from the solar system, and yet others impact the giant planets. In addition, some Jupiter-family comets evolve back into Centaurs (*Hahn and Bailey,* 1990; *Horner et al.,* 2004). Unfortunately, it is impossible to determine from numerical simulations alone whether a given Centaur was a Jupiter-family comet in the past.

Centaurs probably contribute to the near-Earth object (NEO) population. One study finds approximately 6% of the NEO population ultimately comes from the Kuiper belt (*Morbidelli et al.,* 2002). Another study finds a Centaur becomes an Earth-crossing object for the first time about every 880 yr (*Horner et al.,* 2004). Although the percentage of NEOs with a history as a Centaur is small, their potential as hazards is important. Specifically, most NEOs are col-

lision fragments and are significantly smaller than 10 km in diameter. If a large Centaur, like Chiron or Pholus, were to cross Earth's orbit, the debris and dust from a fragmentation could create problems in the space near Earth (*Hahn and Bailey,* 1990).

The number of Centaurs and their total mass is a significant component of the solar system. An analysis of the number of Centaur discoveries in a wide-field optical survey suggests there are about 10^7 Centaurs with diameters larger than 2 km and about 100 Centaurs with diameters larger than 100 km (*Sheppard et al.,* 2000). The same analysis estimates the total mass of Centaurs at about 10^{-4} $M_\oplus$. For comparison, the total mass of main belt asteroids is about 10^{-3} $M_\oplus$ (*Davis et al.,* 2002).

A considerable amount of what we know about the physical and chemical properties of Centaurs comes from photometry. An analysis of groundbased optical photometry and Spitzer Space Telescope infrared photometry for a sample of the known Centaurs yields diameters ranging from 32 to 259 km and albedos ranging from 2% to 18% (see the chapter by Stansberry et al.). Optical lightcurves yield Centaur periods of rotation ranging from 4.15 to 13.41 hours (see the chapter by Sheppard et al.). The evolution of Pholus' lightcurve over a decade suggests it has a highly nonspherical shape, i.e., it has axial ratios of 1.9:1:0.9 (*Farnham,* 2001; *Tegler et al.,* 2005). If Pholus is a strengthless rubble pile and its nonspherical shape is due to rotational distortion, then its axial ratios and period of rotation (9.980 ± 0.002 h) indicate it has a density of 0.5 g cm^{-3}, suggestive of an ice-rich and porous interior (*Tegler et al.,* 2005).

The volatile-rich nature of Centaurs is evident in near-infrared spectra of four Centaurs. In particular, H_2O-ice and possibly CH_3OH-ice bands are seen in the spectrum of Pholus (*Cruikshank et al.,* 1998). In addition, H_2O-ice bands are seen in the spectra of (10199) Chariklo (*Brown et al.,* 1998), (32522) Thereus (*Licandro and Pinilla-Alons,* 2005), and (83982) Crantor (*Doressoundiram et al.,* 2005a).

Further evidence for the volatile-rich nature of Centaurs comes from images of four additional Centaurs. 2060 Chiron (*Meech and Belton,* 1990), 166P/NEAT (*Bauer et al.,* 2003a), 167P/CINEOS (*Romanishin et al.,* 2005), and (60558) Echeclus (*Choi et al.,* 2006) all exhibit comae. Some Centaurs (by our dynamical definition) with comae have comet names (e.g., 167P/CINEOS) and others have both a Centaur and a comet name (e.g., 60558 Echeclus is also known as 174P/Echeclus). Echeclus is on both the Centaur and short-period-comet lists of the Minor Planet Center. At r = 12.9 AU, Echeclus displayed an extraordinarily large and complex coma (Fig. 1). At such large distances, it's too cold for sublimation of H_2O-ice to drive the coma formation. It is possible much more volatile molecular ices such as CO-ice and CO_2-ice are driving the coma formation in Centaurs. Alternatively, *Blake et al.* (1991) suggest the formation of a CH_3OH clathrate from a mixture of amorphous H_2O and CH_3OH can result in the exhalation of excess CH_3OH in a burst of activity at large heliocentric distances.

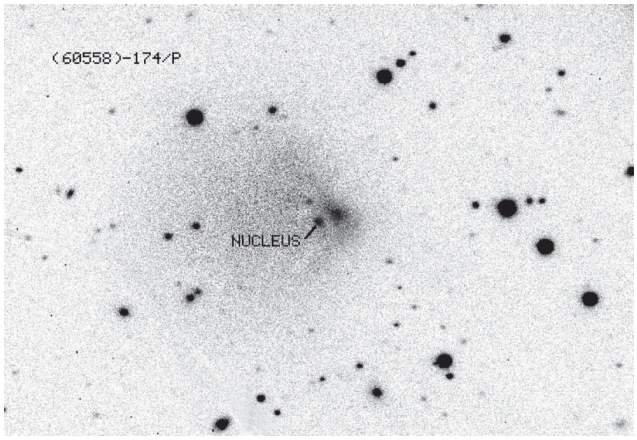

Fig. 1. A 360-s R-band image of Echeclus and a complex coma structure. The image was obtained on 2006 April 2.3 UT with the Vatican Advanced Technology 1.8-m telescope on Mt. Graham, Arizona. It has dimensions of 285 arcsec by 195 arcsec. North is toward the top and east is toward the left. Echeclus is at the position marked "nucleus," with an R magnitude of 20.1. The complex coma structure includes a low-surface brightness coma of diameter 2 arcmin that is centered 1 arcmin east of Echeclus, R = 16, and a higher-surface brightness condensation about 12 arcsec in diameter centered about 7 arcsec west of Echeclus, R = 17.9. Echeclus was at r = 12.9 AU. If the complex coma structure is due to a second object at the position of the higher-surface brightness condensation, the relationship between the two objects is not clear, nor is why the second object appears to exhibit a coma and Echeclus does not exhibit a coma.

Perhaps the most surprising discovery about Centaurs concerns their surface colors. Centaurs and KBOs should exhibit a range of surface colors because (1) solar and cosmic radiation should redden the surfaces, and (2) occasional impacts by smaller objects should puncture the radiation reddened crusts and expose interior, pristine, gray ices (*Luu and Jewitt,* 1996). Surprisingly, measurements of the optical B–R colors of Centaurs divide into two distinct color populations (*Peixinho et al.,* 2003, *Tegler et al.,* 2003).

This chapter describes the two color populations and their statistical significance. Then, we use the two populations to try and constrain important formation and evolution processes in the outer solar system.

2. COLOR MEASUREMENTS

2.1. Objects with Coma

Besides the four Centaurs with coma mentioned above (2060 Chiron, 166P/NEAT, 167P/CINEOS, and 60558 Echeclus), there are five additional objects that are often classified as comets because they exhibit coma: the orbits of 29P/Schwassmann-Wachmann 1, 39P/Oterma, 165P/LINEAR, C/2001 M10 (NEAT), and P/2004 A1 (LONEOS) are consistent with our definition of a Centaur, q > 5.2 AU and a < 30.1 AU. Indeed, Oterma's close encounter with Jupiter in 1963 moved its perihelion distance from that of a Ju-

piter-family comet at 3.4 AU to that of a Centaur at 5.47 AU (see discussion by *Bauer et al.,* 2003a).

It is quite difficult to measure the surface colors of active Centaurs as it requires observations during unpredictable windows of inactivity when the surfaces are not embedded in coma gas and dust. In general, Centaurs with activity appear to exhibit surfaces that absorb sunlight with nearly equal efficiency between wavelengths of 5500 and 6500 Å. In other words, Centaurs with activity display surfaces with nearly solar colors, $(V–R)_{\odot} = 0.36$ (*Bauer et al.,* 2003a). A notable exception is 166P/NEAT, which had an unusually red color during a recent period of activity, (V–R) = 0.95 ± 0.02 (*Bauer et al.,* 2003a). Regardless of whether the red color is due to the surface or coma, 166P/NEAT is one of the reddest Centaurs known. Measurements of additional active Centaurs are essential to determine the effect of coma activity on surface colors and evolution.

2.2. Objects Without Coma

2.2.1. B–R colors. Two teams independently and simultaneously discovered that Centaurs exhibit two different slopes in their reflectance spectra between 4500 and 6500 Å, i.e., they exhibit two distinct B–R color populations (*Peixinho et al.,* 2003; *Tegler et al.,* 2003). An examination of their samples finds 15 objects in common. The mean difference between the 15 pairs of measurements is 0.02 mag, i.e., the two teams find essentially the same colors for the same objects. The excellent agreement says two things. First, the two color measurements for each Centaur were obtained at random rotational phases, so it appears Centaurs do not in general exhibit large color variations over their surfaces. Second, there are no apparent systematic effects in the photometry of either team that could yield the observed bimodality in the B–R color.

The excellent agreement between the two teams suggests it is reasonable to combine the two samples into a single sample of 26 Centaurs (Table 1). For each of the 15 overlap objects, an average value is given in Table 1 where the two individual measurements are weighted by the inverse square of their corresponding uncertainties. The orbital elements come from the Deep Ecliptic Survey (*www.lowell.edu/users/buie/kbo/kbofollowup.html*). Objects in the table are ordered from grayer, i.e., solar-type colors (B–R = 1.03 on the Kron-Cousins system), to redder colors. Colors for Chiron and Echeclus come at times when they had little or no coma contamination.

Figure 2 shows a histogram of the B–R colors in Table 1. The gray population has 1.0 < B–R < 1.4, and the red population has 1.7 < B–R < 2.1. Notice there are no objects with 1.4 < B–R < 1.7 among the sample of 26 Centaurs.

2.2.2. V–R and R–I colors. A V–R and R–I color survey of 24 Centaurs does not exhibit two color populations; see Fig. 1 of *Bauer et al.* (2003b). The color dichotomy

TABLE 1. Centaur colors and orbital elements.

Name	Number	Prov Des	B–R	Source*	a	Q	q	i	e	H
	95626	2002 GZ_{32}	1.03 ± 0.04	TRC	23.03	28.02	18.03	15.02	0.217	6.84
Chiron	2060	1977 UB	1.04 ± 0.05	Pei	13.49	18.57	8.40	6.99	0.377	6.16
		2002 DH_5	1.05 ± 0.07	Pei	22.19	30.41	13.96	22.46	0.371	10.20
Bienor	54598	2000 QC_{243}	1.12 ± 0.03	avg	16.48	19.76	13.20	20.73	0.199	7.52
	119315	2001 SQ_{73}	1.13 ± 0.02	TRC	17.51	20.60	14.42	17.42	0.176	9.57
Hylonome	10370	1995 DW_2	1.15 ± 0.06	avg	25.11	31.36	18.86	4.14	0.249	8.93
		2000 FZ_{53}	1.17 ± 0.05	TRC	23.67	34.99	12.34	34.90	0.478	11.41
Thereus	32532	2001 PT_{13}	1.18 ± 0.01	TRC	10.71	12.86	8.55	20.34	0.202	8.67
	63252	2001 BL_{41}	1.20 ± 0.03	avg	9.79	12.71	6.87	12.47	0.298	11.51
Okyrhoe	52872	1998 SG_{35}	1.21 ± 0.02	avg	8.41	10.99	5.84	15.62	0.306	10.93
		2003 WL_7	1.23 ± 0.04	TRC	20.14	25.35	14.94	11.17	0.258	8.98
Asbolus	8405	1995 GO	1.23 ± 0.05	avg	18.16	29.46	6.86	17.61	0.622	9.07
	120061	2003 CO_1	1.24 ± 0.04	TRC	20.87	30.79	10.94	19.73	0.476	8.81
Pelion	49036	1998 QM_{107}	1.25 ± 0.04	avg	20.14	22.96	17.32	9.36	0.140	10.37
Chariklo	10199	1997 CU_{26}	1.26 ± 0.04	avg	15.82	18.50	13.13	23.38	0.170	6.40
Echeclus	60558	2000 EC_{98}	1.38 ± 0.04	avg	10.71	15.63	5.80	4.35	0.458	9.50
Elatus	31824	1999 UG_5	1.70 ± 0.02	avg	12.74	18.02	7.46	5.59	0.414	9.88
Amycus	55576	2002 GB_{10}	1.79 ± 0.03	avg	25.01	34.81	15.21	13.35	0.392	7.45
	88269	2001 KF_{77}	1.81 ± 0.04	TRC	25.87	31.96	19.77	4.36	0.236	9.49
Crantor	83982	2002 GO_9	1.85 ± 0.02	avg	19.34	24.65	14.04	12.78	0.274	8.60
Cyllarus	52975	1998 TF_{35}	1.86 ± 0.05	avg	26.41	35.56	16.26	12.62	0.384	9.25
	121725	1999 XX_{143}	1.86 ± 0.07	Pei	17.98	26.30	9.66	6.77	0.463	8.53
Nessus	7066	1993 HA_2	1.88 ± 0.06	Pei	24.83	37.85	11.81	15.63	0.524	9.54
		2001 XZ_{255}	1.92 ± 0.07	TRC	16.03	16.59	15.47	2.61	0.035	11.13
		1994 TA	1.92 ± 0.06	avg	16.76	21.84	11.67	5.40	0.303	11.43
Pholus	5145	1992 AD	2.04 ± 0.07	avg	20.25	31.81	8.69	24.71	0.571	6.89

*Source: TRC = *Tegler et al.* (2003); Pei = *Peixinho et al.* (2003). Avg = weighted average of colors from TRC and Pei.

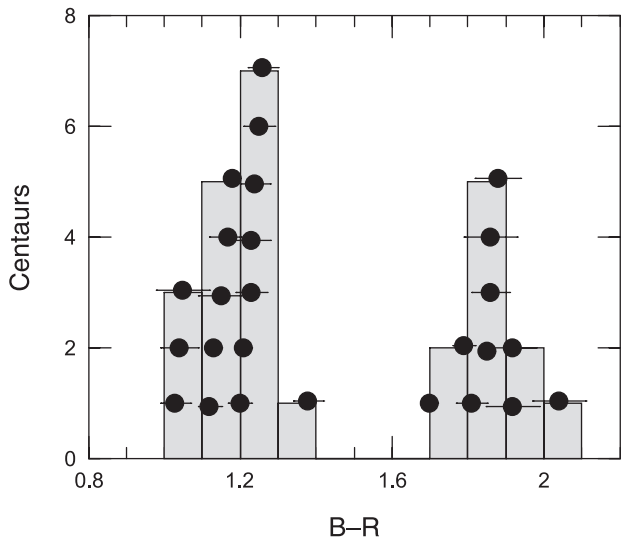

Fig. 2. Histogram of Centaur B–R colors in Table 1. Centaurs appear to divide into two distinct color populations, one with solar to slightly red colors, 1.0 < B–R < 1.4, and the other with red colors, 1.7 < B–R < 2.1. For reference, the Sun has B–R = 1.03.

appears largest in optical surveys that include short-wavelength B-band measurements.

2.2.3. H–K colors. In a near-infrared color survey of 17 Centaurs, *Delsanti et al.* (2006) found two interesting results. First, they found that the objects appear to divide into two color groups on a H–K vs. B–R color-color plot (see their Fig. 3), suggesting a correlation between the absorbers at B-band and H- or K-band.

Second, they found Centaurs with the reddest B–R colors display H–K colors bluer than the Sun (H–K = 0.06). Delsanti et al. suggest that an absorption feature between 1.7 and 2.2 μm is responsible for the bluer than solar colors. The H_2O-ice band at 2.2 μm is a prime candidate as three of the objects exhibit the band in spectroscopic observations. However, H_2O-ice does not absorb near 4500 Å and so it cannot be responsible for the B–R colors.

3. STATISTICAL TEST OF B–R AND H–K BIMODALITY

3.1. Discussion of Dip Test

A visual inspection of Fig. 2 in this chapter or Fig. 3 in *Delsanti et al.* (2006) suggest that Centaurs divide into two B–R and two H–K color populations; however, it is essential to quantify the statistical significance of the apparent divisions. So, what's a good statistical test to apply to Centaur colors?

Present knowledge of Centaur colors is insufficient to justify the assumption of a particular probability distribution, e.g., a normal distribution. Therefore, it is safest to use nonparametric tests that do not assume a particular probability distribution. Furthermore, tests based on bins (e.g., *Jewitt and Luu,* 2001) and Monte Carlo simulations (e.g., *Hainaut and Delsanti,* 2002; *Tegler and Romanishin,* 2003) are very dependent on the way the bins are chosen.

The dip test (*Hartigan and Hartigan,* 1985) is a nonparametric test that does not assume a particular probability distribution and does not require binning data. It is designed to test for one population (unimodality) vs. two populations (bimodality) using monotone regression.

The dip test finds the best fitting unimodal function and measures the maximum difference (*dip*) between that function and the empirical distribution of the sample. This *dip* approaches zero for samples from a unimodal distribution and approaches a positive number for a multimodal distribution. The probability that such a *dip* is not due to pure chance may be obtained from the tables published by *Hartigan and Hartigan* (1985). The dip test and tables for significance levels are also available in the R statistical package (*www.r-project.org*). The dip test is similar to the Kolmogorov Test (*Kolmogorov,* 1933).

3.2. Result of Dip Test on B–R Colors

Application to the dip test in the R package to the sample of N = 26 B–R colors in Table 1 and Fig. 2 results in *dip* = 0.11597, implying that the B–R color distribution is bimodal at a confidence level of CL = 99.5%. There are 10 objects in the red group and 16 in the gray group.

3.3. Result of the Dip Test on H–K Colors

An application of the dip test to 17 H–K Centaur colors indicates there is only a 32% probability that the H–K color distribution is bimodal (*Delsanti et al.,* 2006). On the other hand, application of the Kolmogorov test to the H–K and B–R colors in their Fig. 3 suggests there is a 96.4% probability that there are two H–K and B–R populations. It will be interesting to see what increasing the size of the Delsanti et al. H–K sample does to the statistical probability of two H–K color populations.

4. DIFFERENCES BETWEEN TWO COLOR POPULATIONS

Since the dip test finds the B–R color distribution is bimodal at the 99.5% level, it is natural to look for additional differences between the two color populations in the hope that they will lead to a physical explanation for the two color populations. The Wilcoxon rank sum test is a nonparametric test that does not require data binning (*www.r-project.org*). It provides a way to test the statistical significance of any differences.

4.1. Orbital Elements and Absolute Magnitude

The three left panels in Fig. 3 display semimajor axis, a, aphelion distance, Q, and perihelion distance, q, vs. B–R color for the 26 Centaurs. As there is no apparent correlation between color and a, Q, or q within a color population, the median value of each orbital element within a color

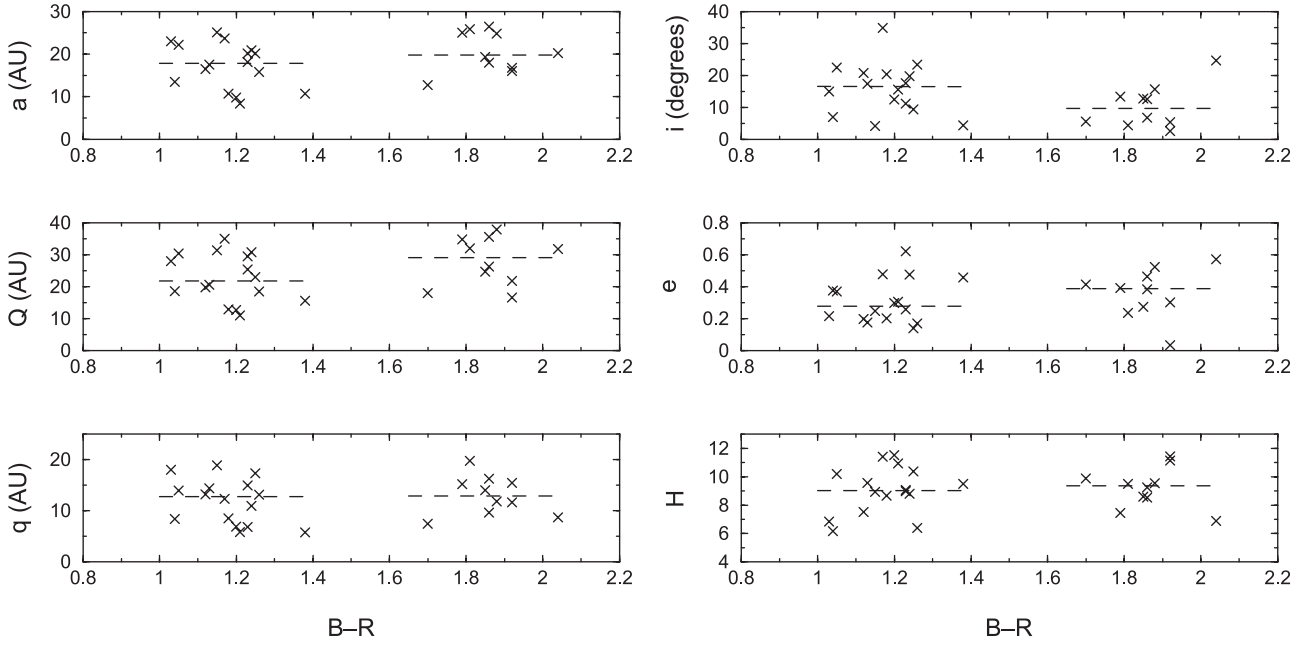

Fig. 3. There are no major differences between the gray and red Centaur values of a, Q, q, i, and e as well as absolute magnitude H. The dashed lines in each panel indicate the median value of a, Q, q, i, e, or H for the gray and red populations. The greatest probability of a difference between the two populations occurs for inclination angle. A Wilcoxon rank sum test says the probability that the gray and red Centaurs have the same inclination angle distribution is 10%.

population is marked with a dashed line extending across the color range of the population. It appears red Centaurs have slightly larger orbits than gray Centaurs (median red a = 19.8 AU, median gray a = 17.8 AU). Interestingly, V–R and R–I color measurements suggest that redder Centaurs exhibit slightly larger semimajor axis values (see Fig. 6 in *Bauer et al.,* 2003b). It also appears that redder Centaurs extend farther from the Sun than gray Centaurs (median red Q = 29.1 AU, median gray Q = 21.8). The red and gray Centaur populations appear to have virtually identical values for q.

The three right panels in Fig. 3 display inclination angle, i, eccentricity, e, and absolute visual magnitude, H, vs. B–R color. The i distribution is most interesting. All but one of the red Centaurs lie at an inclination angle lower than the median inclination angle of the gray population, suggesting that red Centaurs have significantly lower inclination angles than gray Centaurs. Red Centaurs appear to have slightly larger eccentricities than gray Centaurs. V–R and R–I color measurements appear to exhibit the same eccentricity pattern (*Bauer et al.,* 2003b). The absolute magnitudes of the red and gray populations appear virtually identical.

Despite the apparent patterns visible to the eye in Fig. 3, application of the Wilcoxon rank sum test finds no statistically significant difference between the gray and red Centaur values of a, Q, q, i, e, and H. The parameter exhibiting the most statistically significant difference between the gray and red Centaurs is inclination angle. The Wilcoxon test indicates the probability of red and gray Centaurs having the same inclination angle distribution is 10%.

4.2. Albedo

Figure 4 displays albedo measurements from Spitzer Space Telescope and groundbased optical photometry (see the chapter by Stansberry et al.) vs. B–R color for 15 Centaurs (Table 1). It appears gray Centaurs exhibit lower albedos than red Centaurs. The Wilcoxon rank sum test indicates that the probability of gray and red Centaurs having the same albedo distribution is only 1%. In other words, the median albedos of gray and red Centaurs exhibit a statistically significant difference. Stansberry et al. apply the Spearman test to albedos and slopes of optical spectra (colors) and find the likelihood of a correlation is 98%.

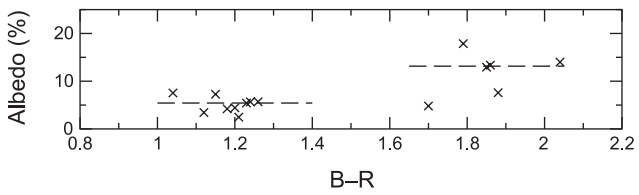

Fig. 4. Gray Centaurs exhibit smaller albedos than red Centaurs. The two dashed lines indicate the median value of albedo for the gray and red populations. A Wilcoxon rank sum test says the probability that the gray and red Centaurs have the same albedo distribution is only 1%. The median albedos of gray and red Centaurs exhibit a statistically significant difference. Albedos are from the chapter by Stansberry et al. and B–R colors come from Table 1.

5. COLORS OF OTHER SOLAR SYSTEM OBJECTS

Some or all of the solar system objects below may have a dynamical link to Centaur objects. Therefore, it is natural to compare their colors to Centaur colors in the hope the comparison will result in a reason for the two Centaur B–R color populations.

5.1. Comet Nuclei

Dynamical simulations suggest some Centaurs evolve into Jupiter-family comets and some Jupiter-family comets evolve into Centaurs (see section 1). B–R colors exist for 12 Jupiter-family comet nuclei (*Jewitt and Luu,* 1990; *Luu,* 1993; *Meech et al.,* 1997; *Delahodde et al.,* 2001; *Jewitt,* 2002; *Li et al.,* 2006) and two Oort cloud comet nuclei (*Jewitt,* 2002; *Abell et al.,* 2005). Observing bare comet nuclei requires observations at large heliocentric distances so that the nuclei are not shrouded in sublimating gas and dust. However, at large heliocentric distances the nuclei are faint and difficult to observe. From a comparison of Figs. 5a and 5b, it is apparent comet nuclei only overlap the gray Centaur population. None of the 14 nuclei exhibit colors similar to the red Centaur population.

5.2. Jupiter Trojans

Recent dynamical simulations suggest Trojan asteroids (located 60° ahead and behind Jupiter at the L4 and L5 Lagrangian points) may have formed well beyond Jupiter and were subsequently captured by Jupiter early in the history of the solar system (*Morbidelli et al.,* 2005). (See the chapter by Dotto et al. for a review of current ideas on the formation of Jupiter Trojans.) From a comparison of Figs. 5a and 5c, it is apparent Trojan asteroids overlap the gray Centaur population. None of the 26 Trojans in Fig. 5c (*Fornasier et al.,* 2004) exhibit colors similar to the red Centaur population.

5.3. Irregular Satellites

Irregular satellites of the jovian planets have larger inclination angles, eccentricities, and semimajor axes than regular satellites. These orbital characteristics suggest irregular satellites were captured by their parent planets. Figure 5d is a B–R histogram of 1 neptunian (*Schaefer and Schaefer,* 2000), 8 saturnian (*Grav et al.,* 2003), and 12 jovian satellites. Again, the colors of these irregular satellites overlap the gray Centaur population. B–R colors for the uranian satellites (Caliban and Sycorax) do not appear in Fig. 5d because colors in the literature are inconsistent (*Maris et al.,* 2001; *Rettig et al.,* 2001; *Romon et al.,* 2001).

5.4. Neptune Trojans

Neptune Trojans were likely captured in the L4 and L5 Lagrangian regions during or shortly after Neptune's formation (see discussion by *Sheppard and Trujillo,* 2006). Four Neptune Trojans are now known and they have essentially gray colors (Fig. 5e) (Sheppard and Trujillo).

5.5. Kuiper Belt Objects

The chapter by Doressoundiram et al. contains a thorough discussion of KBO colors. Here the focus is on KBO dynamical classes that are possible sources of Centaurs and their B–R colors for comparison to Centaur B–R colors.

5.5.1. Plutinos. The presence of objects at a = 39.6 AU in the 2:3 mean-motion resonance with Neptune, Plutinos, may be the result of sweeping resonance capture of the migrating planets (*Hahn and Malhotra,* 2005). *Romanishin and Tegler* (2007) have combined their B–R colors with those in the literature to produce a B–R histogram with 41 Plutinos (Fig. 5f). Plutino colors span the range of the two Centaur color populations, but their distribution appears continuous rather than dividing into two populations. Application of the dip test yields only a 70% probability of two color populations.

5.5.2. Cold classical Kuiper belt objects. Dynamically cold classical KBOs are on orbits with $q > 40$ AU, $42 < a < 45$ AU, $e < 0.1$, and $i < 10°$. They may have formed close to or at their current location. They are dominated by extremely red surface colors (*Tegler and Romanishin,* 2000; *Jewitt and Luu,* 2001; *Tegler et al.,* 2003; *Peixinho et al.,* 2004; *Doressoundiram et al.,* 2005b). A histogram of B–R colors for a sample of 25 cold classical KBOs is given in Fig. 5g. The B–R color measurements in the figure come from 17 papers in the literature. Only 1 out of 25 objects overlaps the color range of gray Centaurs.

5.5.3. Scattered disk objects. Scattered disk objects (SDOs) are thought to have been scattered by Neptune, or another giant planet, onto orbits with large inclinations, $i > 15°$, large eccentricities, $e > 0.3$, and large semimajor axes, $a > 45$ AU. A histogram of 17 SDOs in Fig. 5h exhibits a lack of red surface colors. The B–R color measurements in the figure come from 22 papers in the literature.

6. POSSIBLE EXPLANATIONS

The possible processes responsible for two distinct B–R color populations of Centaurs and the colors of objects with dynamical links to the Centaurs divide into two groups: evolutionary and primordial.

6.1. Evolutionary

Evolutionary models carry the implicit assumption that KBO subsurface material is pristine whereas surface material reddens, darkens, and becomes refractory as a result of continual bombardment by solar radiation (e.g., ultraviolet photons and solar wind particles).

In addition, evolutionary models assume random and occasional collisions puncture radiation-reddened crusts and expose pristine, volatile, subsurface material. Such a model explains the range of colors seen among KBOs irrespective of dynamical class (*Luu and Jewitt,* 1996). Surface tempera-

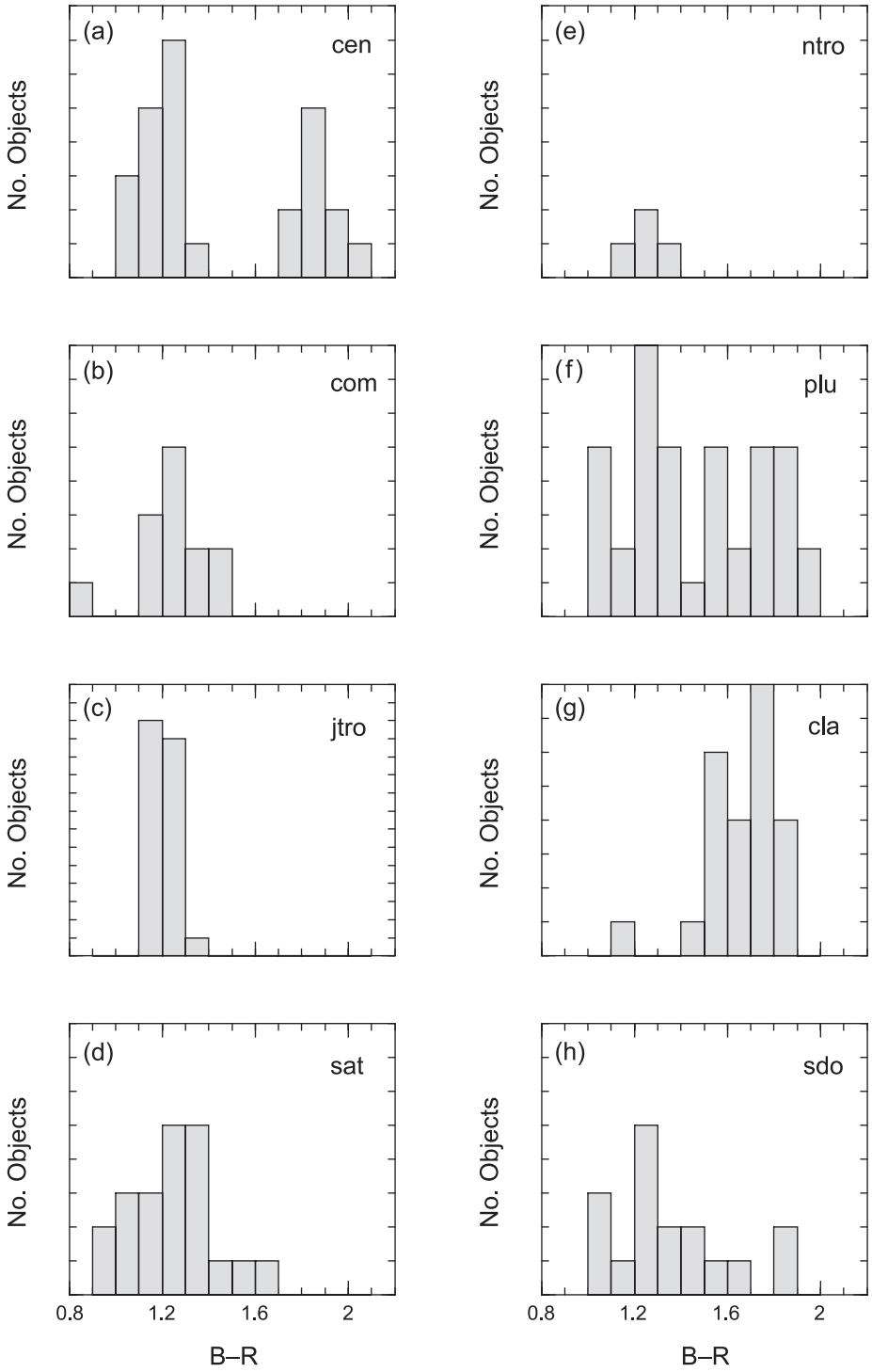

Fig. 5. Histograms of B–R colors for outer solar system objects. The objects in panels **(b)**–**(h)** are ordered in increasing semimajor axis: (**a)** Centaur objects; (**b)** comet nuclei; (**c)** jovian Trojans; (**d)** irregular satellites of Jupiter, Saturn, and Neptune; (**e)** neptunian Trojans; (**f)** Plutinos; (**g)** cold classical KBOs; (**h)** scattered disk objects. Notice that Centaurs are the only class of objects interior to the Kuiper belt that exhibit B–R > 1.7. Each tick mark on the y-axis corresponds to one object.

tures are probably too low in the Kuiper belt for most molecular ices to sublimate (25–50 K).

As some KBOs make their way onto Centaur orbits and thereby get closer to the Sun, their evolution is probably dominated by radiation-reddening and sublimation. Because Centaurs reside in a less-densely populated region than the Kuiper belt, collisions are probably not as important as they are for KBOs.

In evolutionary models, red KBOs with thick, global, reddish crusts become red Centaurs that are able to resist solar heating of subsurface material. In other words, red Centaurs have ancient surfaces. Gray KBOs with surfaces

recently reworked by impacts become gray Centaurs. The red crusts of these objects are largely destroyed, making it easy for them to sublimate volatile icy material (e.g., CO and N_2 ices). *Doressoundiram et al.* (2005b) suggest there are no Centaurs with intermediate colors because when KBOs with small patches of exposed interior material and intermediate colors become Centaurs, they quickly sublimate and either coat their surfaces with gray debris or destroy more red crust and so give these objects a more globally gray color.

Burial of red crusts by sublimation debris is a reasonable explanation of the lack of red surface colors among comet nuclei, Trojan asteroids, and irregular satellites (Fig. 5). *Jewitt* (2002) first put forth such a mechanism to explain the lack of red colors among comet nuclei.

It is possible to test the sublimation mechanism as an explanation of Centaur colors. Specifically, observations of KBOs with intermediate colors should exhibit B–R color variations as they rotate.

6.2. Primordial

It is possible that KBOs and Centaurs retain some signature of their primordial colors. For example, perhaps at a heliocentric distance slightly smaller than 40 AU CH_4 went from condensing in a H_2O-ice rich clathrate to condensing as pure CH_4 (*Lewis,* 1972). Whereas the loss of CH_4 from from a clathrate surface results in a lag made up of colorless H_2O-ice crust, a pure CH_4-ice crust provides much material for alteration into red organic compounds, even if there was a substantial amount of CH_4 sublimation. So perhaps objects that formed less than 40 AU from the Sun originally had gray surface colors and objects that formed beyond 40 AU had red surface colors. CH_4-ice bands are seen in spectra of (134340) Pluto (*Cruikshank et al.,* 1976; *Fink et al.,* 1980; *Grundy and Fink,* 1996), Neptune's satellite Triton, which may be a captured KBO (*Cruikshank et al.,* 1993), (136199) Eris (*Brown et al.,* 2005), and (136472) 2005 FY9 (*Licandro et al.,* 2006; *Tegler et al.,* 2007). It is also possible that CH_3OH could provide the carbon and hydrogen for radiation-induced reddening events.

A complication to looking for such a primordial color signature is that all KBOs and Centaur objects (with the possible exception of low-inclination classical KBOs and a few resonant objects) have been scattered by Neptune from their original orbits. For example, a dynamical simulation predicts that as Neptune migrated outward it scattered objects originally 25 AU from the Sun onto orbits of the present-day SDOs, high-inclination classical KBOs, and high-inclination Plutinos. In contrast, low-inclination classical KBOs remained far enough away from Neptune that they weren't perturbed much by the planet (*Gomes,* 2003).

If the CH_4 chemistry idea and the dynamical simulation are correct, SDOs, high-inclination classical KBOs, and high-inclination Plutinos formed less than 40 AU from the Sun and they should exhibit gray surface colors, whereas low-inclination KBOs formed more than 40 AU from the Sun and they should exhibit red surface colors. In general, observations support these patterns (*Tegler et al.,* 2003).

How would such a mechanism explain two distinct color populations of Centaurs? Centaurs have short orbital lifetimes, and so their color distribution is dominated by recent Neptune scatterings of KBOs. Perhaps Neptune is now sufficiently far enough from the Sun and hence close enough to the low-inclination classical belt that it now scatters some red low-inclination classical KBOs onto Centaur orbits. Remember, there is a hint in Fig. 3 that the red Centaurs have lower orbital inclinations than the gray Centaurs. Although it may be difficult or impossible to use current day orbital parameters of Centaurs to say much about orbital parameters before their scatterings, inclination angle may be the one orbital parameter that retains some memory (*Levison and Duncan,* 1997). So, perhaps the two color populations of Centaurs are pointing to two separate source regions in the Kuiper belt (e.g., gray Centaurs come from SDOs and red Centaurs come from low-inclination classical belt objects).

7. CONCLUSIONS

It is clear that Centaur objects exhibit two distinct B–R color populations. Although there are ideas as to why there are two color populations, further theoretical and observational work is necessary to determine whether the dichotomy is primordial or due to evolutionary processes.

Acknowledgments. S.C.T. and W.R. acknowledge support from NASA Planetary Astronomy grant NNG 06GI38G. N.P. acknowledges support from the European Social Fund and the Portuguese Foundation for Science and Technology (SFRH/BPD/18729/2004).

REFERENCES

Abell P. A. and 10 colleagues (2005) Physical characteristics of comet nucleus C/2001 OG108 (LONEOS). *Icarus, 179,* 174–194.

Bauer J. M., Fernández Y. R., and Meech K. J. (2003a) An optical survey of the active Centaur C/NEAT (2001 T4). *Publ. Astron. Soc. Pac., 115,* 981–989.

Bauer J. M., Meech K. J., Fernández Y. R., Pittichova J., Hainaut O. R., Boehnhardt H., and Delsanti A. C. (2003b) Physical survey of 24 Centaurs with visible photometry. *Icarus, 166,* 195–211.

Blake D., Allamandola L, Sandford S., Hudgins D., and Friedemann F. (1991) Clathrate hydrate formation in amorphous cometary ice analogs in vacuo. *Science, 254,* 548–551.

Brown M. E., Trujillo C. A., and Rabinowitz D. L. (2005) Discovery of a planetary-sized object in the scattered Kuiper belt. *Astrophys. J. Lett., 635,* L97–L100.

Brown R. H., Cruikshank D. P., Pendleton Y., and Veeder G. J. (1998) Identification of water ice on the Centaur 1997 CU26. *Science, 280,* 1430–1432.

Choi Y. J., Weissman P. R., and Polishook D. (2006) (60558) 2000 EC_{98}. *IAU Circular 8656.*

Cruikshank D. P., Pilcher C. B., and Morrison D. (1976) Pluto — Evidence for methane frost. *Science, 194,* 835–837.

Cruikshank D. P., Roush T. L, Owen T. C., Geballe T. R., de Bergh C., Schmitt B., Brown R. H., and Bartholomew M. J. (1993) Ices on the surface of Triton. *Science, 261,* 742–745.

Cruikshank D. P. and 14 colleagues (1998) The composition of Centaur 5145 Pholus. *Icarus, 135,* 389–407.

Davis D. R., Durda D. D., Marzari F., Bagatin A. C., and Gill-Hutton R. (2002) Collisional evolution of small body populations. In *Asteroids III* (W. F. Bottke Jr. et al., eds.), pp. 545–558. Univ. of Arizona, Tucson.

Delahodde C. E., Meech K. J., Hainaut O. R., and Dotto E. (2001) Detailed phase function of comet 28P/Neujmin 1. *Astron. Astrophys., 376,* 672–685.

Delsanti A., Peixinho N., Boehnhardt H., Barucci A., Merlin F., Doressoundiram A., and Davies J. K. (2006) Near-infrared properties of Kuiper belt objects and Centaurs: Final results from the ESO large program. *Astron J., 131,* 1851–1863.

Doressoundiram A., Barucci M. A., Tozzi G. P., Poulet F., Boehnhardt H., de Bergh C., and Peixinho N. (2005a) Spectral characteristics of the trans-Neptunian object (55565) 2002 AW197 and the Centaurs (55576) 2002 GB10 and (83982) 2002 GO9: ESO large program on TNOs and Centaurs. *Planet. Space Sci., 53,* 1501–1509.

Doressoundiram A., Peixinho N., Doucet C., Mousis O., Barucci M. A., Petit J. M., and Veillet C. (2005b) The Meudon multicolor survey (2MS) of Centaurs and trans-Neptunian objects: Extended dataset and status on the correlations reported. *Icarus, 174,* 90–104.

Farnham T. L. (2001) The rotation axis of Centaur 5145 Pholus. *Icarus, 152,* 238–245.

Fink U., Smith B. A., Johnson J. R., Reitsema H. J., Benner D. C., and Westphal J. A. (1980) Detection of a CH_4 atmosphere on Pluto. *Icarus, 44,* 62–71.

Fornasier S., Dotto E., Marzari F., Barucci M. A., Boehnhardt H., Hainaut O., and de Bergh C. (2004) Visible spectroscopic and photometric survey of L5 Trojans: Investigation of dynamical families. *Icarus, 172,* 221–232.

Gomes R. S. (2003) The origin of the Kuiper belt high-inclination population. *Icarus, 161,* 404–418.

Grav T., Holman M. J., Gladman B. J., and Aksnes K. (2003) Photometric survey of irregular satellites. *Icarus, 166,* 33–45.

Grundy W. M. and Fink U. (1996) Synoptic CCD spectrophotometry of Pluto over the past 15 years. *Icarus, 124,* 329–343.

Hahn G. and Bailey M. E. (1990) Rapid dynamical evolution of the giant comet Chiron. *Nature, 348,* 132–136.

Hahn J. M. and Malhotra R. (2005) Neptune's migration into a stirred-up Kuiper belt: A detailed comparison of simulations to observations. *Astron J., 130,* 2392–2414.

Hainaut O. R. and Delsanti A. C. (2002) Colors of minor bodies in the outer solar system. A statistical analysis. *Astron. Astrophys., 389,* 641–664.

Hartigan J. A. and Hartigan P. M. (1985) The dip test of unimodality. *Ann. Stat., 13,* 70–84.

Horner J., Evans N. W., and Bailey M. E. (2004) Simulations of the population of Centaurs — I. The bulk statistics. *Mon. Not. R. Astron. Soc., 354,* 798–810.

Jewitt D. C. (2002) From Kuiper belt object to cometary nucleus: The missing ultrared matter. *Astron. J., 123,* 1039–1049.

Jewitt D. C. and Luu J. X. (1990) CCD spectra of asteroids. II — The Trojans as spectral analogs of cometary nuclei. *Astron. J., 100,* 933–944.

Jewitt D. C. and Luu J. X. (2001) Colors and spectra of Kuiper belt objects. *Astron. J., 122,* 2099–2114.

Kolmogorov A. N. (1933) About the empirical determination of a distribution law. *Giornale dell' Istituto Italiano degli Attuari, 4,* 83–91.

Kowal C. T. (1979) Chiron. In *Asteroids* (T. Gehrels, ed.), pp. 436–439. Univ. of Arizona, Tucson.

Levison H. F. and Duncan M. J. (1997) From the Kuiper belt to Jupiter-family comets: The spatial distribution of ecliptic comets. *Icarus, 127,* 13–32.

Lewis J. S. (1972) Low temperature condensation from the solar nebula. *Icarus, 16,* 241–252.

Li J.-Y., A'Hearn M. F., McFadden L. A., Sunshine J. M., Crockett C. J., Farnham T. L., Lisse C. M., Thomas P. C., and the Deep Impact Science Team (2006) Deep Impact photometry of the nucleus of Comet 9P/Tempel 1. In *Lunar and Planetary Science XXXVII,* Abstract #1839. Lunar and Planetary Institute, Houston (CD-ROM).

Licandro J. and Pinilla-Alonso N. (2005) The inhomogeneous surface of Centaur 32522 Thereus (2001 PT13). *Astrophys. J. Lett., 630,* L93–L96.

Licandro J., Pinilla-Alonso N., Pedani M., Oliva E., Tozzi G. P., and Grundy W. M. (2006) The methane ice rich surface of large TNO 2005 FY9: A Pluto-twin in the trans-Neptunian belt? *Astron. Astrophys., 445,* L35–L38.

Luu J. X. (1993) Spectral diversity among the nuclei of comets. *Icarus, 104,* 138–148.

Luu J. and Jewitt D. (1996) Color diversity among the Centaurs and Kuiper belt objects. *Astron. J., 112,* 2310–2318.

Maris M., Carraro G., Cremonese G., and Fulle M. (2001) Multicolor photometry of the Uranus irregular satellites Sycorax and Caliban. *Astron. J., 121,* 2800–2803.

Meech K. J. and Belton M. J. S. (1990) The atmosphere of Chiron. *Astron. J., 100,* 1323–1338.

Meech K. J., Bauer J. M., and Hainaut O. R. (1997) Rotation of comet 46P/Wirtanen. *Astron. Astrophys., 326,* 1268–1276.

Morbidelli A., Bottke W. F., Froeschle C., and Michel P. (2002) Origin and evolution of near Earth objects. In *Asteroids III* (W. F. Bottke Jr. et al., eds.), pp. 409–422. Univ. of Arizona, Tucson.

Morbidelli A., Levison H. F., Tsiganis K., and Gomes R. (2005) Chaotic capture of Jupiter's Trojan asteroids in the early solar system. *Nature, 435,* 462–465.

Peixinho N., Doressoundiram A., Delsanti A., Boehnhardt H., Barucci M. A., and Belskaya I. (2003) Reopening the TNO color controversy: Centaurs bimodality and TNOs unimodality. *Astron. Astrophys., 410,* L29–L32.

Peixinho N., Boehnhardt H., Belskaya I., Doressoundiram A., Barucci M. A., and Delsanti A. (2004) ESO large program on Centaurs and TNOs: Visible colors — final results. *Icarus, 170,* 153–166.

Rettig T. W., Walsh K., and Consolmagno G. (2001) Implied evolutionary differences of the jovian irregular satellites from a BVR color survey. *Icarus, 154,* 313–320.

Romon J., de Bergh C., Barucci M. A., Doressoundiram A., Cuby J. G., Le Bras A., Doute S., and Schmitt B. (2001) Photometric and spectroscopic observations of Sycorax, satellite of Uranus. *Astron. Astrophys., 376,* 310–315.

Romanishin W. and Tegler S. C. (2007) Statistics and optical colors of KBOs and Centaurs. In *Statistical Challenges in Modern Astronomy IV* (E. Feigelson and G. J. Babu, eds.), in press. Astronomical Society of the Pacific, San Francisco.

Romanishin W., Tegler S. C., Boattini A., de Luise F., and di Paola A. (2005) Comet C/2004 PY_{42}. *IAU Circular 8545.*

Schaefer B. E. and Schaefer M. W. (2000) Nereid has complex large-amplitude photometric variability. *Icarus, 146,* 541–555.

Scotti J. V. (1992) 1992 AD. *IAU Circular 5434.*

Sheppard S. S. and Trujillo C. A. (2006) A thick cloud of Neptune Trojans and their colors. *Science, 313,* 511–514.

Sheppard S. S., Jewitt D. C., Trujillo C. A., Brown M. J. I., and Ashley M. C. B. (2000) A wide-field CCD survey for Centaurs and Kuiper belt objects. *Astron. J., 120,* 2687–2694.

Tegler S. C. and Romanishin W. (2000) Extremely red Kuiper belt objects in near-circular orbits beyond 40 AU. *Nature, 407,* 979.

Tegler S. C. and Romanishin W. (2003) Resolution of the Kuiper belt color controversy: Two distinct color populations. *Icarus, 161,* 181–191.

Tegler S. C., Romanishin W., and Consolmagno G. (2003) Colors patterns in the Kuiper belt: A possible primordial origin. *Astrophys. J. Lett., 599,* L49–L52.

Tegler S. C., Romanishin W., Consolmagno G. J., Rall J., Worhatch R., Nelson M., and Weidenschilling S. (2005) The period of rotation, shape, density, and homogeneous surface color of the Centaur 5145 Pholus. *Icarus, 175,* 390–396.

Tegler S. C., Grundy W. M., Romanishin W., Consolmagno G. J., Mogren K., and Vilas F. (2007) Optical spectroscopy of the large Kuiper belt objects 136472 (2005 FY9) and 136108 (2003 EL61). *Astron. J., 133,* 526–530.

Tiscareno M. S. and Malhotra R. (2003) The dynamics of known Centaurs. *Astron. J., 126,* 3122–3131.